University Department of Pharmaceutical Sciences[1], Utkal University, Bhubaneswar Institute of Pharmacy and Technology[2], Salipur, Cuttack, Orissa, India

Design and evaluation of a nanoparticulate system prepared by biodegradable polymers for oral administration of protein drugs

S. Kumar Sahu [1], A. Kumar Prusty [2]

The present work was about the preparation of nanoparticles by a complex coacervation process using the biodegradable polymers Chitosan and sodium alginate and to evaluate their suitability for oral administration of proteins. Bovine serum albumin (BSA) was used as a model protein for incorporation into the nanoparticulate system. The prepared BSA-loaded nanoparticles were characterized for size, morphology, zeta potential, BSA encapsulation efficiency and subsequent release kinetics. The physicochemical characters of the prepared nanoparticles depend mostly on polymers mass ratio, pH of the reaction medium and BSA loading concentration. The minimum average size of empty nanoparticles were found to be 339.80 ± 02.20 nm and the BSA loaded nanoparticles prepared under varying conditions had average sizes in the range of 473.67 ± 18.75 nm to 751.33 ± 6.81 nm, and exhibit a high positive zeta potential. The SEM image showed spherical shaped nanoparticles. By increasing the concentration of BSA from 0.1 mg/ml to 2.8 mg/ml the loading capacity of the nanoparticulate system was increased whereas the encapsulation efficiency was decreased. The results suggest that the nanoparticulate system is a potential carrier for delivering protein drugs.

1. Introduction

The oral delivery of many therapeutic proteins is difficult due to their large size, hydrophilicity, and instability (Lee and Yamamoto 1990). Protein instability is one of the major reasons why biologically active proteins are administered preferably as injection rather than taken orally (Wang 1999). The main hurdles for the stability of orally adminisdesed proteins are the acid catalyzed degradation in stomach, poor permeability across the gastrointestinal mucosa and first pass metabolism during transfer across the absorption barrier in the liver. Biological products must overcome these barriers for efficient delivery into the blood stream (Xing et al. 2003). An ideal nanoparticle delivery system for biological products can be developed by using materials that are biodegradable and biocompatible (Lee and Kang 2006). Mucoadhesive polymers are preferred as carrier materials for the preparation of nanoparticles as they facilitate interaction of the nanocarrier with the intestinal mucosa, facilitating its transport to the underlying epithelium. The properties of nanoparticles are quite different from those of polymer solutions or large polymer devices, for example chitosan solution hardly diffuses through the mucus membrane whereas chitosan as a nanoparticle carrier can easily penetrate to the mucosa (Takeuchi et al. 2001). Naturally occurring polysaccharides like chitosan and alginate are having immense advantages to be used as primary material in forming carriers for therapeutic protein molecules (George and Abraham 2006). Chitosan is derived from chitin by partial deacetylation and is a copolymer of glucosamine and N-acetyl-*d*-glucosamine linked together by β(1,4) glycosidic bonds. Chitosan is a biodegradable polymer and degraded

into N-acetyl glucosamine by lysozymes present in the body. N-acetyl glucosamine is metabolized and excreted out of the body as carbon dioxide via the glycoprotein synthetic pathway. Chitosan is having wide applications in the pharmaceutical field, due to its favorable biological properties such as biodegradability, biocompatibility, low toxicity, haemostatic, bacteriostatic, fungistatic, anticarcinogenic, and anticholesteremic properties (Hejazi and Amiji 2003). The backbone of glucosamine units present in Chitosan has a high density of amine groups, permitting strong electrostatic interactions with proteins being negatively charged at neutral pH (Mao et al. 2004; Gan and Wang 2007). Chitosan as a carrier for nanoparticles imparts a positive surface charge and increases the contact time of nanoparticles with the epithelium and enhance absorption via the paracellular transport pathway through the tight junctions. Alginate is a water soluble polysaccharide composed of alternating blocks of 1–4 linked α-L-guluronic and β-D-mannuronic acid residues. Alginate is extracted from brown sea weeds and has mucoadhesive, biodegradable, and biocompatible properties like that of chitosan (Gombotz and Wee 1998; Li et al. 2008). The nanoparticles are prepared using biodegradable polymers by methods like ionic gelation, complex coacervation, emulsion cross-linking, and spray-drying, but ionic gelation (also known as ionotropic gelation) and complex coacervation are preferred as these are mild processes and retain the stability of incorporated proteins. Preparation of nanoparticles by ionic gelation and complex coacervation are almost similar. Howevers, an electrolyte is used in ionic gelation whereas an oppositely charged ionic polymer is used in complex coacervation (Calvo et al. 1997; De and Robinson 2003; Agnihotri et al. 2004; Sinha
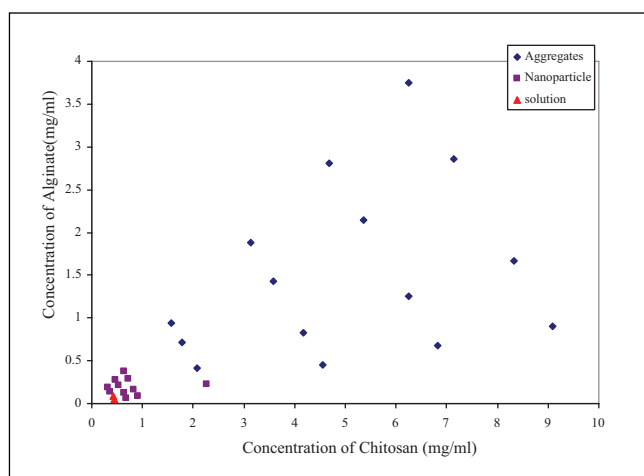
Fig. 1: Identification of nanoparticles domain formation

(A)

(B)

Fig. 2: Scanning electron microscopy image of (A) empty nanoparticles
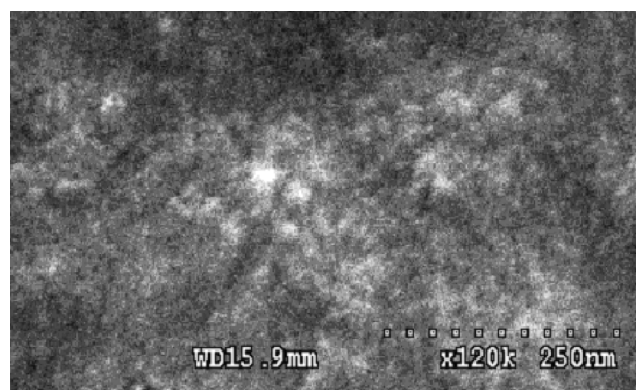(B) BSA-loaded nanoparticle

et al. 2004). The main objective of present work was to prepare nanoparticles by using the polycation chitosan and the polyanion alginate by complex coacervation process and to evaluate their physicochemical properties and efficacy for entrapment and controlled release of the standard protein bovine serum albumin.

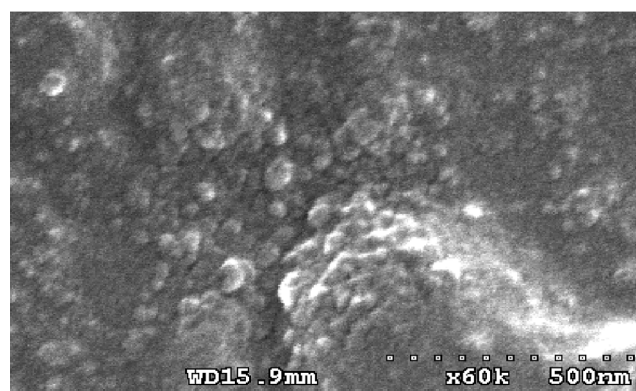## 2. Investigations, results and discussion

Nanoparticles were prepared spontaneously without using high temperature, organic solvents, or sonication. The nanoparticles showed a good protein loading capacity as well as a pH dependent continuous release of the entrapped standard protein for several days. These properties made the nanoparticulate system a promising protein carrier.

2.1. Conditions for the formation of nanoparticles

The linkages created between carboxyl groups of alginate and the amino groups of chitosan were responsible for the success of the gelation process. It was observed that a concentration of chitosan between 0.312 and 2.273 mg/ml and sodium alginate between 0.068 and 0.375 mg/ml produced the opalescence zone (Fig. 1). The particle size of nanoparticles was dependent on both Chitosan and Sodium alginate concentrations. The average size of smallest nanoparticles formed was 391.80 ± 6.89 nm when 0.286 mg/ml of sodium alginate were added to 0.714 mg/ml of chitosan with an average zeta potential of 31.37 ± 3.69 mV and a PDI of 0.162 ± 0.04 (Table 1). The SEM image of empty nanoparticles was observed as solid and consistent spherical structure (Fig. 2A).

2.2. Effect of pH, calcium chloride and stirring time on the formation of nanoparticles

As chitosan was solubilised under acidic (pH 3.3) conditions there might be a chance of precipitation upon addition to alginate solution (pH 6.9), therefore less chitosan might be available for particle formation. As the pKa of Chitosan is 6.5, addition of chitosan solution (pH 3.3) to alginate solution (pH 6.9) would result in unprotonated amine groups, therefore chitosan could not participate in ionic interactions with alginate. The few protonated groups available for interaction would result in weaker electrostatic interactions with the alginate, leading to larger particle size. Using an alginate solution with a lower pH resolves these problems by allowing a stronger interaction between chitosan and alginate, leading to the formation of more compact nanoparticles (Calvo et al. 1997; Mohanraj et al. 2006). It was observed that smaller nanoparticles were formed when

Table 1: **Effect of weight ratio of chitosan and sodium alginate on physicochemical properties of empty nanoparticles**

Conc. of chitosan (mg/ml)	Conc. of alginate (mg/ml)	Final volume (ml)	Particle size (nm ± SD)	Zeta potential (mV ± SD)	PDI ± SD
2.273	0.227	5.5	1627.0 ± 86.82	41.17 ± 1.07	0.526 ± 0.05
0.625	0.375	8.0	599.25 ± 13.17	33.40 ± 2.16	0.225 ± 0.02
0.714	0.286	7.0	391.80 ± 6.89	31.37 ± 3.69	0.162 ± 0.04
0.833	0.167	6.0	427.65 ± 10.21	35.43 ± 3.38	0.223 ± 0.02
0.909	0.091	5.5	409.75 ± 12.17	39.43 ± 1.25	0.273 ± 0.05
0.469	0.281	8.0	443.25 ± 16.94	29.73 ± 0.64	0.390 ± 0.06
0.536	0.214	7.0	403.30 ± 9.81	33.06 ± 1.10	0.180 ± 0.03
0.625	0.125	6.0	572.50 ± 45.79	33.53 ± 2.34	0.478 ± 0.02
0.682	0.068	5.5	412.83 ± 191.16	37.66 ± 2.52	0.320 ± 0.05
0.312	0.187	8.0	482.00 ± 20.99	24.33 ± 0.58	0.417 ± 0.02
0.357	0.143	7.0	458.77 ± 12.34	24.76 ± 2.93	0.494 ± 0.03

Table 2: Effects of pH change on formation of empty nanoparticles

Chitosan pH	Alginate pH	Particle size (nm ± SD)	Zeta potential (mV ± SD)	PDI ± SD
3.3	6.9	391.80 ± 06.89	31.37 ± 3.69	0.162 ± 0.04
4.0	6.5	384.65 ± 07.52	31.49 ± 0.83	0.156 ± 0.01
4.5	6.0	371.38 ± 10.43	31.35 ± 1.06	0.157 ± 0.01
5.0	5.5	350.10 ± 08.70	32.03 ± 1.21	0.148 ± 0.01
5.3	5.3	339.80 ± 02.20	32.50 ± 0.99	0.137 ± 0.01
6.0	5.0	378.02 ± 23.95	30.85 ± 0.65	0.158 ± 0.02

Table 3: BSA concentration and its effect on loaded nanoparticles

BSA conc. (mg/ml)	Particle Size (nm ± SD)	Zeta potential (mV ± SD)	PDI ± SD	Encapsulation Efficiency ± SD	Loading % ± SD
0.1	473.67 ± 18.75	27.40 ± 1.37	0.160 ± 0.02	77.22 ± 3.50	19.11 ± 1.17
0.4	509.33 ± 9.29	22.33 ± 0.86	0.153 ± 0.05	35.68 ± 5.13	25.68 ± 1.06
0.8	592.67 ± 9.02	20.60 ± 0.62	0.153 ± 0.02	24.79 ± 1.27	27.29 ± 0.42
1.2	681.67 ± 8.74	18.66 ± 0.65	0.193 ± 0.02	20.65 ± 0.74	32.89 ± 0.31
1.6	693.67 ± 19.86	17.47 ± 0.54	0.167 ± 0.03	18.41 ± 0.80	36.45 ± 0.51
2.0	718.67 ± 7.02	16.07 ± 0.65	0.190 ± 0.04	14.92 ± 0.46	41.33 ± 1.37
2.4	729.67 ± 5.03	15.63 ± 0.42	0.153 ± 0.01	11.4 ± 0.46	43.05 ± 1.39
2.8	751.33 ± 6.81	14.64 ± 0.36	0.180 ± 0.05	10.17 ± 1.72	44.01 ± 0.38

both sodium alginate and chitosan solutions had a pH of 5.3 (Table 2). At pH 5.3 the carboxyl groups of alginate were ionized and the amine groups of chitosan were protonated, making an optimum condition for interaction resulting in complex formation. It was suggested that presence of calcium ions was important to maintain the alginate gel network during reaction with chitosan resulting in better nanoparticles (Rajaonarivony et al. 1993). In our study it was observed that use of calcium increased the particle size. The nanoparticle preparation was carried out for different time periods starting from 30 min to 24 h and the particle size was determined but the result did not show any appreciable change in particle size. Therefore it can be concluded that nanoparticle formation was rapid and reorganization of the polymers was not occurring over time.

2.3. Characterisation of BSA loaded nanoparticles

The particle size of loaded nanoparticles increased with increasing amounts of BSA used. The smallest particles with particle sizes of 473.67 ± 18.75 nm were formed with 0.1 mg/ml of BSA. The Zeta potential of loaded nanoparticles was decreased with increasing quantity of BSA used with a maximum value of 27.4 ± 1.37 mV (Table 3). The encapsulation efficiency was decreased (Fig. 3A) whereas the loading percentage was increased (Fig. 3B) by increasing the amount of BSA. Highest encapsulation efficiency was 77.22 ± 3.50 when the amount of BSA used was 0.1 mg/ml and the highest loading percentage was 44.01 ± 0.38 when the amount of BSA was 2.8 mg/ml (Table 3). The isoelectric point of BSA was 4.8, therefore at higher pH, i.e., at 5.3 (pH of nanoparticle formation medium) BSA was negatively charged and interacted with positive amino groups present in chitosan, leading to high BSA entrapment within the nanoparticle. Therefore it could be concluded that protein–polysaccharide electrostatic interaction was the main factor responsible for protein association in the nanoparticles (Bhumkar and Pokharkar 2006). The zeta potential of BSA loaded nanoparticles was changed slightly both in sign and magnitude as compared to empty nanoparticle might be due to ionic interaction of negatively charged BSA with positively charged chitosan. The SEM image of BSA loaded nanoparticles was observed as solid and consistent spherical structure as the empty nanoparticles (Fig. 2B).

### 2.4. FTIR spectra of the nanoparticles

The FTIR spectrum of chitosan showed peaks at $1652 \, \text{cm}^{-1}$ and $1309 \, \text{cm}^{-1}$ corresponding to amide I and amide III bonds respectively and a strong protonated amino peak at $1544 \, \text{cm}^{-1}$ corresponding to chitosan formation by partial N-deacetylation of chitin. The two peaks at $995 \, \text{cm}^{-1}$ and $1155 \, \text{cm}^{-1}$ correspond to the saccharide structure of chitosan. The peak at $1456 \, \text{cm}^{-1}$ indicates symmetrical deformation of the methyl group (Bhattarai et al. 2006).The FT-IR spectrum of sodium alginate showed carboxyl peaks near $1610 \, \text{cm}^{-1}$ corresponding to symmetric stretching vibration and at $1465 \, \text{cm}^{-1}$ corresponding to asymmetric stretching vibration. Due to complex formation between chitosan and sodium alginate during nanoparticle preparation the peak at $1652 \, \text{cm}^{-1}$ of chitosan and the peak at $1610 \, \text{cm}^{-1}$ of sodium alginate disappeared and two new peaks at $1649 \, \text{cm}^{-1}$ and $1572 \, \text{cm}^{-1}$ appeared in the FT-IR spectrum of the nanoparticles (Bhumkar and Pokharkar 2006). The peak at $1465 \, \text{cm}^{-1}$ of Chitosan shifted to $1433 \, \text{cm}^{-1}$ in the nanoparticle and the stretching vibration of hydroxyl group at $3360 \, \text{cm}^{-1}$ in Chitosan shifted to a broad band at $3419 \, \text{cm}^{-1}$ in the nanoparticle. The FTIR spectrum of BSA showed characteristic peaks of acetylamino I group at $1645 \, \text{cm}^{-1}$, acetylamino II at $1522 \, \text{cm}^{-1}$ and acetylamino III at $1292 \, \text{cm}^{-1}$, and a peak at $3340 \, \text{cm}^{-1}$ corresponding to amino functional group (Chun et al. 2007). The acetyl amino I and II peaks of BSA overlapped with the peaks at $1649 \, \text{cm}^{-1}$ and $1572 \, \text{cm}^{-1}$ of empty nanoparticles and resulted in to two new peaks at $1639 \, \text{cm}^{-1}$ and $1547 \, \text{cm}^{-1}$ in the FT-IR spectrum of BSA loaded nanoparticle (Fig. 4).

2.5. Stability of the nanoparticles

The nanoparticles were stored at 4 °C for two months in deionised water, but did not show a marked change in particle size and zeta potential. A small change was observed which might be due to swelling of the nanoparticles by absorption of water (Table 4). Therefore it was confirmed that the nanoparticles were not aggregated and were stable for the stored period in deionised water.

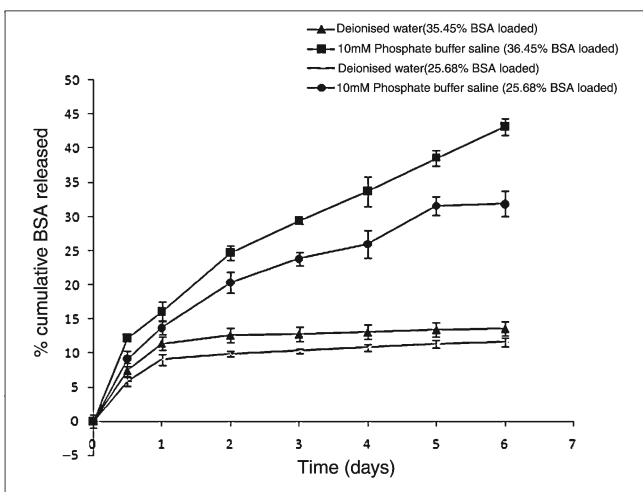### 2.6. In-Vitro release of BSA from the nanoparticles

The *in-vitro* release of BSA from loaded nanoparticles was observed to a greater extent in the release media of high ionic
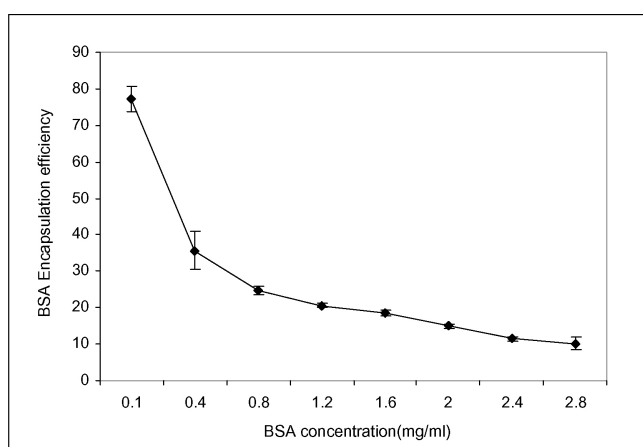
(A)
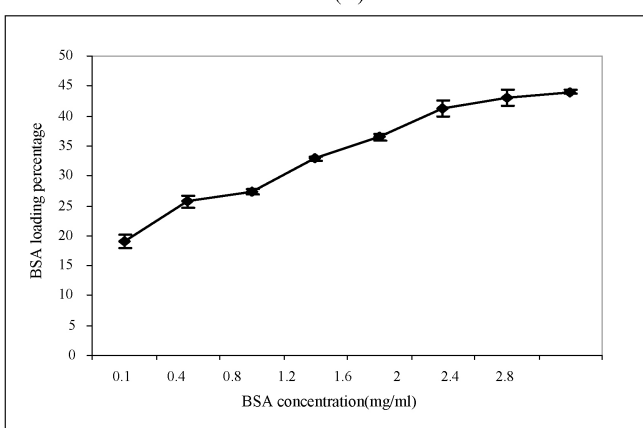
(B)

(C)

Fig. 3: BSA (A) Encapsulation efficiency (B) loading percentage (C) Cumulative release

Fig. 4: FTIR spectra of (A) chitosan, (B) sodium alginate, (C) empty nanoparticle, (D) BSA, (E) BSA loaded nanoparticle

Table 4: Effect of time on stability of nanoparticles

Time (month)	Particle size (nm ± SD)	Zeta potential (mV ± SD)
0	339.80 ± 2.20	32.50 ± 0.99
1/2	345.67 ± 5.03	32.05 ± 0.45
1	351.33 ± 3.05	30.57 ± 0.83
2	356.33 ± 6.81	29.65 ± 1.34

strength (PBS) as compared to water over the release study period (Fig. 3C). The release study showed that initially there was a burst release may be due to desorption of loosely attached BSA from the surface of the matrix polymers. There was almost no release of BSA from nanoparticles kept in water at the first two time points. Around 31.87 % and 43.20 % of BSA was released from nanoparticles prepared by incorporating 0.4 mg/ml and 1.6 mg/ml BSA respectively in 10 mM phosphate buffer saline over a period of 6 days (Table 5). It might be due to large molecular size of BSA that made it difficult to dissociate via ion exchange and diffusion through the chitosan-alginate matrix structure. It was evident that both the molecular size of the drug and ionic interaction, rather than the pH difference between water and phosphate buffer, affect the rate of BSA released from the nanoparticles (Mohanraj et al. 2006). It was observed that the release rates were 31.87 % and 43.20 % for nanoparticles prepared by incorporating 0.4 mg/ml and 1.6 mg/ml of BSA (Table 5) i.e., the higher the protein loading the higher was the release rate.

Table 5: Cumulative (%) release of BSA from BSA loaded nanoparticles

Time (days)	% Release of BSA from A ± SD	% Release of BSA from B ± SD	% Release of BSA from C ± SD	% Release of BSA from D ± SD
0.5	07.45 +/− 0.78	12.21 ± 0.36	05.88 +/− 0.67	09.18 ± 1.06
1	11.42 +/− 1.08	16.06 ± 1.51	09.01 +/− 0.84	13.72 ± 1.06
2	12.64 +/− 0.18	24.69 ± 1.10	09.91 +/− 0.35	20.36 ± 1.56
3	12.78 +/− 0.29	29.36 ± 0.45	10.32 +/− 0.28	23.79 ± 0.97
4	13.08 +/− 0.18	33.67 ± 2.21	10.81 +/− 0.45	26.00 ± 2.05
5	13.44 +/− 0.43	38.59 ± 1.10	11.30 +/− 0.59	31.59 ± 1.43
6	13.59 +/− 0.46	43.20 ± 1.20	11.60 +/− 0.65	31.87 ± 2.21

A: 36.45% BSA loaded nanoparticle in water, B: 36.45% BSA loaded nanoparticle in 10mM PBS, C: 25.68% BSA loaded nanoparticle in water, D: 25.68% BSA loaded nanoparticle in 10mM PBS.
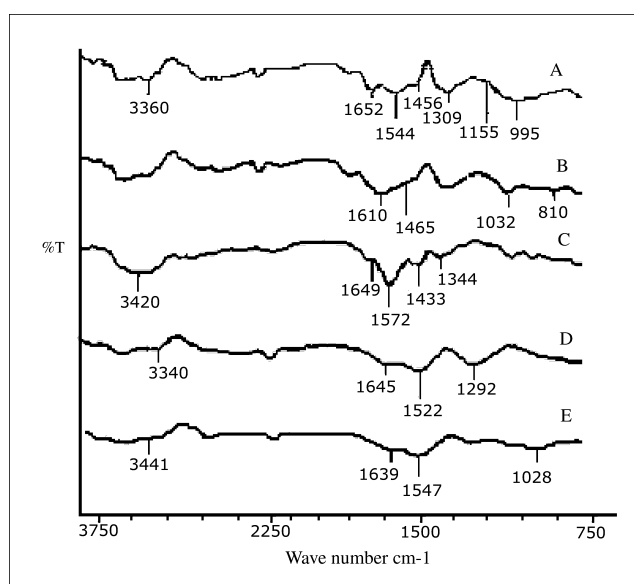
Table 6: Estimated parameters and release mechanism of BSA loaded nanoparticles

Different conc. of BSA loaded nanoparticles	r^2		k	n	Order of release
	Higuchi	Koresmeyer			
BSA 0.4 mg/ml in water	0.874	0.874	0.079	0.24	Fickian
BSA 0.4 mg/ml in PBS	0.991	0.991	0.135	0.50	Non-fickian
BSA 1.6 mg/ml in water	0.796	0.796	0.099	0.21	Fickian
BSA 1.6 mg/ml in PBS	0.996	0.996	0.169	0.51	Non-fickian

k: Kinetic constants, n: Diffusional exponent, r: correlation coefficient.

2.7. Release kinetics

The release kinetics from 10 mM PBS fitted well into Korsmeyer equation ($r^2 > 0.99$) and indicated the release of BSA as a combined effect of diffusion as well as erosion from the nanoparticle polymer matrix (Table 6).

3. Experimental

3.1. Materials

Low molecular weight chitosan (50 KDa) was purchased from Aldrich. Low viscosity sodium alginate was purchased from Sigma, bovine serum albumin (BSA); Coomassie Blue G 250 was purchased from Bio-Rad Laboratories. All other solvents and materials used were of analytical grade.

3.2. Preparation of nanoparticles

To know the concentration range of polymers for formation of nanoparticle, varying concentrations like 0.1 %, 0.25 %, 0.5 %, and 1 %w/v of chitosan and sodium alginate were prepared. One gram of chitosan was dissolved in 100 ml of aqueous acetic acid (1.75 %w/v) to obtain 1 %w/v of chitosan, from that other concentrations like 0.5 %, 0.25 %, and 0.1 %w/v of chitosan were prepared by diluting in deionised water. One gram of Sodium alginate was dissolved in 100 ml of deionised water to obtain 1 %w/v of sodium alginate solution from that other concentrations like 0.5 %, 0.25 %, and 0.1 %w/v of sodium alginate were prepared by diluting with deionised water. Variable volumes of sodium alginate solution like 0.5, 1, 2, and 3 ml were added to 5 ml of respective concentrations of chitosan solution and stirred by a magnetic stirrer at room temperature for 30 min. (Rajaonarivony et al. 1993; Calvo et al. 1997; Mohanraj et al. 2006).

3.2.1. Effect of pH, calcium chloride and stirring time on nanoparticles

The particular concentration of chitosan and sodium alginate producing nanoparticles of smallest size was further investigated at various pH values, by addition of calcium chloride and increasing stirring time to optimize the conditions for nanoparticle formation (Douglas and Tabrizian 2005). Different pH samples of chitosan and alginate solution were mixed and stirred by a magnetic stirrer for 30 min. To the optimized protocol for preparation of nanoparticle measured amount of calcium chloride solution was added dropwise with stirring. The optimized protocol for preparation of nanoparticles was further investigated by increasing the time of stirring. The physicochemical properties of nanoparticles formed by the above changes were determined.

3.2.2. Preparation of BSA loaded nanoparticles

Bovine serum albumin (BSA) was used as a standard protein to study the encapsulation, loading and release characteristics from the nanoparticulate system. The BSA-loaded nanoparticles were prepared by adding various concentrations of BSA like 0.1, 0.4, 0.8, 1.2, 1.6, 2, 2.4, 2.8 mg/ml to 5 ml of 0.1 %w/v chitosan solution with continuous stirring in a magnetic stirrer followed by addition of 2 ml of 0.1 %w/v sodium alginate solution.

3.3. Physicochemical characterization of nanoparticles

3.3.1. size of nanoparticles

Particle size of the nanoparticles was determined by dynamic light scattering on a Malvern Zetasizer Nano-ZS (Malvern Instruments, Malvern, UK). The nanoparticles suspended in purified water to a final concentration of 100 µg/ml. The measurement was done in disposable polystyrene cuvettes at 25 °C with detection angle of 90° and by adjusting the viscosity

and refractive index as 0.8872 cP and 1.33. The average particle size and the polydispersity index (PDI) of three batches of each sample were determined.

3.3.2. Morphology of nanoparticles

The morphological examination of the nanoparticles was performed by Scanning electron microscopy (SEM) using Hitachi S4800. Sample suspension (100 µl) was spread on silicon wafer (SiO$_2$/Si) of size 1 cm × 1 cm and dried at room temperature for overnight. To the dried surface of sample platinum was sputtered and SEM measurement was carried out.

3.3.3. Zeta potential of nanoparticles

Zeta potential was determined by electrophoretic light scattering measurements in a disposable polycarbonate capillary cell by using a Malvern Zetasizer and Particle Analyzer 5000 (Malvern Instruments). The sample concentration was made to 20 µg/ml for measurement of zeta potential. To provide sufficient ionic background, measurements were performed in 1 mM sodium chloride solution.

3.3.4. Identification of nanoparticle constituents

Empty and loaded nanoparticles were analyzed using a Shimadzu 8400S, FT-IR spectrophotometer. The samples were lyophilized, gently mixed with 100 mg of micronized potassium bromide powder and compressed into a disc shaped holder (Sarmento et al. 2006; Li et al. 2008). For each spectrum a 256-scan interferogram was collected with a 4 cm^{-1} resolution in the mid-infrared region at room temperature.

3.3.5. Stability of the nanoparticles

The prepared nanoparticles were suspended in deionised water (1 mg/ml) and stored at room temperature (Freitas and Muller 1999; Douroumis and Fahr 2007). Particle size and zeta potential were determined at different time intervals.

3.4. Physiological characterization of BSA loaded nanoparticles
3.4.1. Size, morphology and zeta potential of loaded nanoparticles

The BSA loaded nanoparticles were investigated for size, morphology and zeta potential by the same protocol as followed in case of empty nanoparticles.

3.4.2. Loading and entrapment efficiency of BSA in the nanoparticles

The amount of BSA entrapped in the nanoparticles was calculated as the difference between the total amount of BSA added to the nanoparticle formation medium and the amount of free BSA remaining in the supernatant. The preparation mixture was centrifuged at 15000 rpm at 4 °C for 15 min separating BSA loaded nanoparticles from free BSA remaining in the supernatant. The amount of free BSA in the supernatant was determined by Bradford protein assay. A BSA standard calibration curve was prepared by taking different concentration of BSA added with 5 ml of Bradford reagent and incubated for 5 min at room temperature and absorbance of samples was determined at 595 nm with a spectrophotometer. 0.1 ml of supernatant containing free BSA collected after centrifuging the loaded nanoparticle mixture was mixed with 5 ml of Bradford reagent and incubated for 5 min at room temperature. The absorbance of the incubated sample was measured at 595 nm using a spectrophotometer (Bradford 1976). From a standard calibration curve, the concentration of BSA present in the supernatant was determined. The BSA loading and entrapment efficiency were calculated by using the following equations:

Loading capacity of nanoparticles

$$= \left[\frac{\text{Total amount of BSA - amount of free BSA}}{\text{Weight of nanoparticles}} \right] \times 100 \qquad (1)$$

Incorporation efficiency

$$= \left[\frac{\text{Total amount of BSA-amount of free BSA}}{\text{Total amount of BSA}} \right] \times 100 \qquad (2)$$

3.4.3. In vitro release study of BSA loaded nanoparticles

A weighed amount of BSA loaded nanoparticle suspension was centrifuged at 15000 rpm for 30 min at 4 °C. The supernatant was decanted and the nanoparticles were resuspended and incubated in 5 ml of an aqueous 10 mM phosphate buffer (pH 7.4), and 5 ml of deionised water, each with controlled agitation at 37 °C. The quantity of nanoparticles was adjusted to obtain a BSA concentration of 1 mg/ml per release study. At specific time intervals, samples were centrifuged at 15000 rpm at 4 °C and 5 ml of the supernatant was removed and replaced by an equal volume of fresh medium. The amount of BSA released into the supernatant at various time intervals was determined using Bradford protein assay method (Bradford 1976). All measurements were performed in triplicate. The empty nanoparticles were incubated at 37 °C and analyzed by the same method to act as control.

3.4.4. Release kinetics of BSA from nanoparticles

To analyze the mechanism of BSA released from the nanoparticulate system, the *in-vitro* release data were fitted to following equations:

$$\text{Higuchi's equation}: Q = k_2 t^{1/2} \qquad (3)$$

(Where Q represents percent of drug released at time t, k_2 is the diffusion rate constant.)

$$\text{Korsmeyer equation}: \text{Log}(M_t/M_\infty) = \text{Log } k + n\text{Log}(t) \qquad (4)$$

(Where M_t is the amount of BSA released at time t, M_∞ is the amount of drug released after infinite time, k is release rate constant, and n is the diffusion exponent)
To clarify the release exponent for BSA loaded nanoprticles log value of percentage drug released was plotted against log time. A value of n equals to 0.45 indicates Fickian release and n value in between 0.45 to 0.89 indicates non-fickian or anomalous (combination of both diffusion and erosion controlled) release (Barzegar and Dastmalchi 2007; Islam et al. 2009).

References

Agnihotri SA, Mallikarjuna NN, Aminabhavi TM (2004) Recent advances on Chitosan-based micro- and nanoparticles in drug delivery. J Control Rel 100: 5–28.

Barzegar JM, Dastmalchi S (2007) Kinetic analysis of chlorpropamide dissolution from solid dispersions. Drug Dev Ind Pharm 33: 63–70.

Bhattarai N, Ramay HR, Chou S, Zhang M (2006) Chitosan and lactic acid-grafted Chitosan nanoparticles as carriers for prolonged drug delivery. Int J Nanomed 1: 181–187.

Bhumkar DR, Pokharkar V B (2006) Studies on effect of pH on cross-linking of chitosan with sodium tripolyphosphate: a technical note. APS Pharm Sci Tech 7: E1–E6.

Bradford M (1976) A rapid and sensitive method for the quantitation of microgram quantities of protein utilizing the principle of protein-dye binding. Anal Biochem 72: 248–254.

Calvo P, Remunan-Lopez C, Vila-Jato JL, Alonso MJ (1997) Novel hydrophilic Chitosan-polyethylene oxide nanoparticles as protein carriers. J Appl Polym Sci 63: 125–132.

Chun W, Xiong F, LianSheng Y(2007) Water-soluble chitosan nanoparticles as a novel carrier system for protein delivery. Chinese Sci Bul 52: 883–889.

De S, Robinson D (2003) Polymer relationships during preparation of chitosan-alginate and poly-l-lysine-alginate nanospheres. J Control Rel 89: 101–112.

Douglas K, Tabrizian M (2005) Effect of experimental parameters on the formation of alginate chitosan nanoparticles and evaluation of their potential application as DNA carrier. J Biomater Sci Polymer Edn 16: 43–56.

Douroumis D, Fahr A (2007) Stable carbamazepine colloidal systems using the cosolvent technique. Eur j Pharm Sci 30: 367–374.

Freitas C, Muller R H, (1999) Stability determination of solid lipid nanoparticles (SLN) in aqueous dispersion after addition of electrolyte. J Microencapsulation 16: 59–71.

Gan Q, Wang T (2007) Chitosan nanoparticle as protein delivery carrier—Systematic examination of fabrication conditions for efficient loading and release. Colloids and Surfaces B: Biointerfaces 59: 24–34.

George M, Abraham TE (2006) Polyionic hydrocolloids for the intestinal delivery of protein drugs: alginate and chitosan — a review. J Control Release 114: 1–14.

Gombotz WR, Wee SF (1998)Protein release from alginate matrices. Adv Drug Deliv Rev 31: 267–285.

Hejazi R, Amiji M (2003) Chitosan-based gastrointestinal delivery systems. J Control Release 89: 1–165.

Islam M S, Moghal MM R, Ud Doula AFM S (2009) Effect of physiochemical properties on the release profile of Diltiazem HCl and Naproxen from HPMC and Kollidon SR based Matrix tablets. Indian J Pharm Educ Res 43: 46–54.

Lee D H, Kang I J (2006) Drug delivery system using biodegradable nanoparticles carrier. KONA 24: 159–166.

Lee VHL, Yamamoto A (1990) Penetration and enzymatic barriers to peptide and protein absorption. Adv Drug Deliv Rev 4: 171–207.

Li P, Dai YN, Zhang JP, Wang AQ, Wei Q (2008) chitosan–alginate nanoparticles as a novel drug delivery system for nifedipine. Int J Biomed Sci 4: 3221–3228.

Mao S, Shuai X, Unger F, Simon M (2004) The depolymerization of chitosan: effects on physicochemical and biological properties. Int J Pharm 281: 45–54.

Mohanraj V J, Chen Y, Suresh B (2006) Chitosan based nanoparticles for delivery of proteins and peptides. Indian J Pharm Educ Res 40: 106–115.

Rajaonarivony M, Vauthier C, Courraze G, Puisieux F, Couvreur P (1993) Development of a new drug carrier made from alginate. J Pharm Sci 82: 912–916.

Sarmento B, Ferreira D, Veiga F, Ribeiro A (2006) Characterization of insulin-loaded alginate nanoparticles produced by ionotropic pregelation through DSC and FTIR studies. Carbohydrate Polymers 66: 1–7.

Sinha VR, Singla AK, Wadhawan S (2004) Chitosan microspheres as a potential carrier for drugs. Int J Pharm 27: 41–33.

Takeuchi H, Yamamoto H, Kawashima Y (2001) Mucoadhesive nanoparticulate systems for peptide drug delivery. Adv Drug Deliv Rev 47: 39–54.

Wang W (1999) Instability, stabilization, and formulation of liquid protein pharmaceuticals. Int J Pharm 185: 129–188.

Xing L, Dawei C, Liping X, Rongquing Z (2003) Oral colon specific drug delivery for bee venom peptide: development of a coated calcium alginate gel beads-entrapped liposome. J Control Release 93: 293–300.